

The Ground-State Parity of $N^{14}\dagger$

D. A. BROMLEY

University of Rochester, Rochester, New York

(Received June 16, 1952)

Four-Mev deuterons from the Rochester 27-inch cyclotron have been used to determine the angular distribution of the neutrons from the $C^{13}(d,n)N^{14}$ ground-state reaction for laboratory angles less than 45° . Similar measurements have been made on the $Be^9(d,n)B^{10}$ and $F^{19}(d,n)Ne^{20}$ ground-state reactions, primarily to confirm the applicability of the Butler stripping theory at this energy and with this particular experimental arrangement. Comparison of the experimental results with the predictions of the theory shows that there is a parity change in the $C^{13}(d,n)N^{14}$ and $Be^9(d,n)Ne^{20}$ reactions and no parity change in the $F^{19}(d,n)Ne^{20}$ reaction. Since the C^{14} and C^{13} ground states have been previously shown to have opposite parity, there can be no parity change in the C^{14} beta-decay.

I. INTRODUCTION

THE C^{14} beta-decay is one of the few cases which has not yet been reconciled with modern beta-decay theory. This spectrum has an apparently allowed shape¹ but the $\log ft$ value for the transition² is 9.05, indicating a forbidden transition.

The spins of C^{14} and N^{14} have been measured^{3,4} to be 0 and 1, respectively; hence, the spin change in the transition is known to be 1. Although the shell theories predict that both the C^{14} and N^{14} ground states should have even parity, several authors have suggested a parity change in the transition as a possible explanation for the anomalously long lifetime. If this were the case, the decay could be first forbidden, but with an allowed spectrum shape, for Fermi or Gamow-Teller selection rules.

A similar difficulty had once existed for the Be^{10} beta-decay, since a spin change of 1 and no parity change had been assumed for the transition. Under these conditions an allowed transition would be predicted, whereas the observed spectrum had a shape corresponding to a highly forbidden transition and a $\log ft$ value² of 13.65 indicating a second or third forbidden transition. This difficulty was resolved when the spin change was measured to be 3.⁵

Since the spin change is known for the C^{14} beta-decay, it was considered of interest to determine whether or not a parity change occurs.

The study of the angular distributions of the neutrons and protons from the $C^{13}(d,n)N^{14}$ and $C^{13}(d,p)C^{14}$ ground-state reaction was chosen as a method for determining the N^{14} and C^{14} ground-state parities, since this made possible not only the determination of the relative parities but also the determination of these parities relative to that of C^{12} . In the remainder of this paper, unless otherwise specified, all reactions and parities will

be those corresponding to the ground states of the nuclei in question. The parity of C^{12} will be assumed even. The spin of C^{13} has been measured³ to be $\frac{1}{2}$ and a study of the angular distribution of the protons from the $C^{12}(d,p)C^{13}$ reaction⁶ has shown that C^{12} and C^{13} have opposite parities. The values of the orbital angular momentum which could be transferred to the C^{13} nucleus by the absorbed nucleon were thus limited to 0, 1, and 2 units, and the experimental distributions had only to be compared with the three distributions predicted by the Butler theory⁷ corresponding to these angular momentum transfers. The results of the $C^{13}(d,p)C^{14}$ experiment have been published previously,⁸ and the experimental method will be described elsewhere.⁹ The C^{14} parity was found to be opposite to that of C^{13} , hence even as expected. This paper will describe the $C^{13}(d,n)N^{14}$ experiment.

When this research was begun, it seemed advisable to carry out an experiment to determine the angular distributions of neutrons from two different reactions, one of which would be expected to show a parity change and the other no parity change. The results of this experiment served to check the apparatus and method against the effects of wall-scattering and similar possible sources of error. They also confirmed the applicability of the Butler theory for the relatively low energy deuterons available. The $Be^9(d,n)B^{10}$ and $F^{19}(d,n)Ne^{20}$ reactions were chosen for this experiment on the basis of shell model predictions.

Thick targets were used to give adequate counting rates. Since the Q value for the $C^{12}(d,n)N^{13}$ reaction is -0.26 Mev and that for the $C^{13}(d,n)N^{14}$ reaction is 5.38 Mev,¹⁰ it was simple to discriminate against the neutrons from the first reaction in the carbon target enriched to 53.7 percent in C^{13} (see Appendix I).

⁶ J. Rotblat, Proceedings of the International Conference on Nuclear Physics, Chicago, Sept. 17-22 (1951).

⁷ S. T. Butler, Proc. Roy. Soc. (London) **A208**, 559 (1951).

⁸ D. A. Bromley and L. M. Goldman, Phys. Rev. **86**, 790 (1952). In the caption for Fig. 1 of this letter, it was incorrectly stated that the value $l_p=2$ is excluded for both the $C^{13}(d,n)N^{14}$ and $C^{13}(d,p)C^{14}$ ground-state reactions.

⁹ L. M. Goldman, Doctoral dissertation, to be submitted to the Physics Department, University of Rochester, August, 1952.

¹⁰ Hornyak, Lauritsen, Morrison, and Fowler, Revs. Modern Phys. **22**, 291 (1950).

[†] Presented in part as a post-deadline paper at the Washington meeting of the American Physical Society, May 3, 1952. This work has been supported by the AEC.

¹ L. Feldman and C. S. Wu, Phys. Rev. **75**, 1286 (1949).

² A. M. Feingold, Revs. Modern Phys. **23**, 10 (1951).

³ F. Jenkins, Phys. Rev. **73**, 639 (1948).

⁴ Kusch, Millman, and Rabi, Phys. Rev. **55**, 1176 (1939).

⁵ Gordy, Ring, and Burg, Phys. Rev. **74**, 1191 (1948).

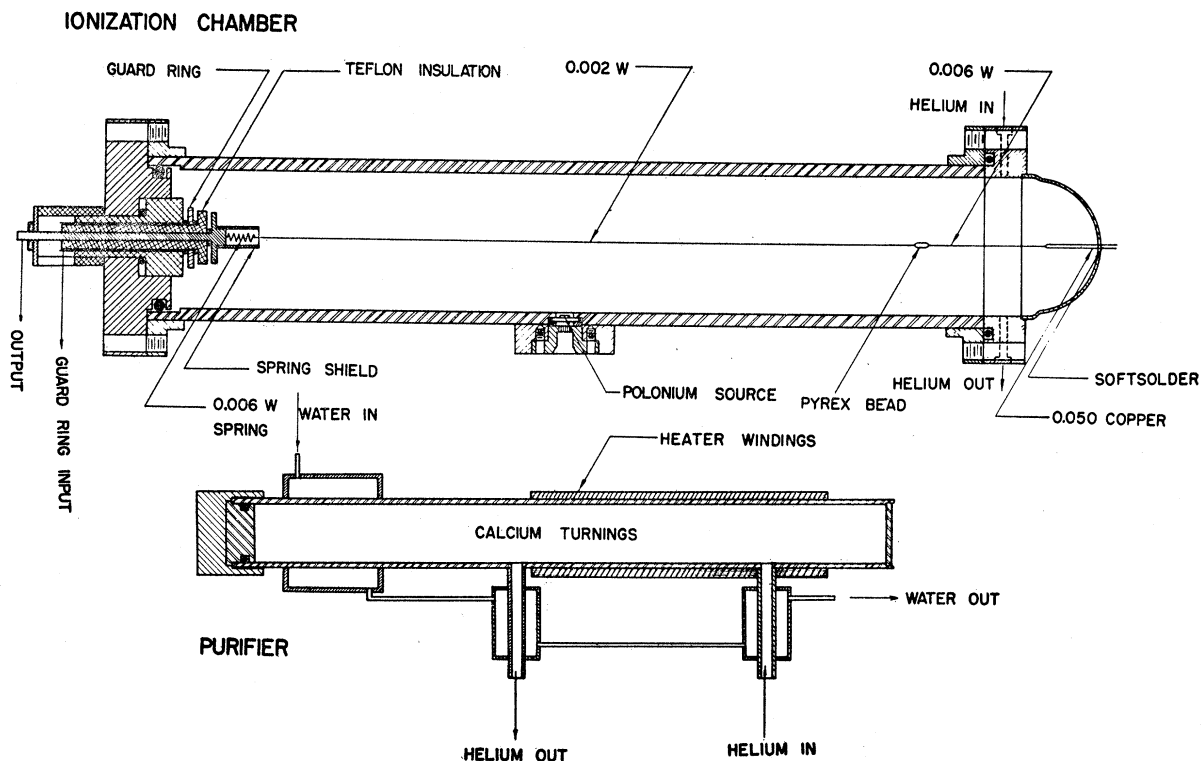


FIG. 1. The ionization chamber and hot calcium purifier. The filling valve and Bourdon pressure gauge which are mounted on the chamber are not shown.

II. EXPERIMENTAL METHOD

A high pressure ionization chamber was chosen as the neutron detector in preference to the more usual photographic plate because it combines the high detection efficiency of the photographic plate with the possibility of continuous checking and the much more rapid rate of obtaining data available with electronic equipment. Helium was used in the chamber rather than hydrogen, because of its greater atomic stopping power, although the maximum energy transfer from the neutrons was 64 percent instead of the 100 percent possible with hydrogen.

Figure 1 shows a section through the ionization chamber. The outer, stainless-steel cylinder is 2 inches in internal diameter and $\frac{3}{16}$ -inch thick. The hemispherical copper cap on the front end of the chamber was made $\frac{1}{16}$ -inch thick to minimize scattering and attenuation of the incident neutrons. A polonium alpha-source was mounted, as shown, for use in calibrating the system and for checking its operation.

When first assembled and filled to 20 atmospheres pressure with tank helium it was found that sufficient contaminants were present to prevent observation of the calibration alpha-pulses.

The helium was passed through a cold trap consisting of a spiral wound from 10 feet of $\frac{1}{8}$ -inch copper tubing which was completely immersed in a Dewar flask of liquid nitrogen. Since sufficient contaminants remained

to prevent energy resolution, a hot-calcium, convection-flow purifier was constructed, as shown in Fig. 1, and attached to the chamber. It was found that 6 to 8 hours treatment with the purifier removed all observable contaminants provided that the helium had been first passed through the cold trap. The purifier was operated continuously to avoid possible poisoning of the helium due to the gradual evolution of gases from the gaskets and walls of the chamber.

Figure 2 shows the experimental arrangement. The circular scattering chamber will be described in detail elsewhere.⁹ The first and last collimator apertures were $\frac{5}{8}$ inch in diameter, and the antiscattering center aperture

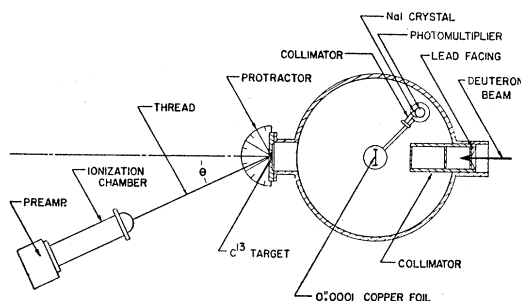


FIG. 2. The experimental arrangement. The scattering chamber is about 15 feet from the cyclotron at the end of the external focusing section. A common vacuum system is used for the cyclotron, exit section, and scattering chamber.

was 41/64 inches in diameter: The apertures were 2 inches apart. The collimated deuteron beam passed through a 0.0001-inch copper foil (1 mg/cm^2), mounted at the center of the scattering chamber and perpendicular to the beam, before striking the thick target. The scintillation counter, set at 132° to the beam direction, detected backscattered deuterons and served as a monitor. This was calibrated by replacing the target-holding plate with a Faraday cage connected to an integrating circuit and measuring the total charge required for a given number of monitor counts.

The targets (see Appendix I) were spring mounted in a well milled at the center of the chamber end plate. The bottom of the well was 0.035 inch thick; hence the neutron scattering and attenuation due to it was negligible.

The ionization chamber was mounted on a simple tripod stand and was moved in an arc of radius 36 inches centered on the target with its axis always pointing toward the target.

Figure 3 is a block diagram of the electronic equipment. All units, with the exception of the 30-channel pulse-height analyzer, are of standard design. The analyzer has been described elsewhere.¹¹ The rf power supply had degenerative regulation both on the input and output of the oscillator and was conveniently adjustable from 500 to 2000 volts. The internal power supply filter was supplemented by an RC external filter and an LC filter mounted directly on the ion chamber. The positive high voltage was applied to the guard ring, which was connected to the central wire through a 10-megohm resistor. The model 500 preamplifier was mounted directly on the chamber in a shield box. The clipping time of the amplifier was adjusted to $20 \mu\text{sec}$ and an RC filter inserted between the two loops of the amplifier set the rise time at $2.5 \mu\text{sec}$.

The amplified photomultiplier output was connected to a second discriminator and scaler for use in monitoring the beam.

Before each run a pulse-height *versus* chamber voltage curve was obtained for the polonium alphas to check on the operating point of the system. A typical curve had a plateau extending from about 850 to 1150 volts, hence the operating voltage was set at 1000 volts. No appreciable change in the chamber characteristics was observed during the experiment.

Before and after each run, 15-minute calibration spectra were taken on the polonium alphas. Figure 4 shows typical spectra. The full curve was taken at the beginning of an eight-hour run and the dashed curve at the end. The increased background at low energies was assumed due to the build-up of neutron-induced beta-activity in the chamber. The longest half-life expected in this activity was that of the 12.9-hour beta-emitter Cu^{64} ; rough measurements of the decrease of this activity were in agreement with this value.

¹¹ Fulbright, McCarthy, and McCutchen, Phys. Rev. **87**, 184 (1952).

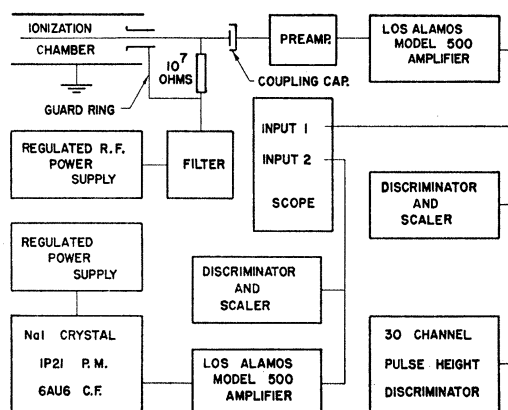


FIG. 3. Block diagram of the electronic equipment.

Since all the pulses of interest corresponded to at least 5 Mev, this activity caused no difficulty.

In any particular run the angle of observation was increased stepwise from 0° to 45° and then reduced stepwise to 0° to check on the internal consistency of the measurements. In all runs used this consistency was within the expected statistical errors. As a check on the angular symmetry of the system, measurements were

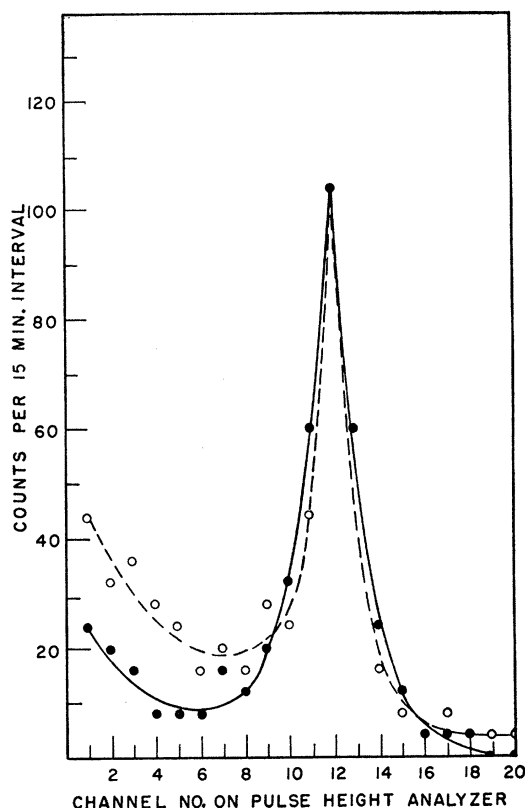


FIG. 4. Polonium alpha-pulse-height spectra. The zero of the distribution is at minus 6 channels. The solid line is the spectrum at the beginning of an 8-hour run; the dashed line is the spectrum at the end of the run.

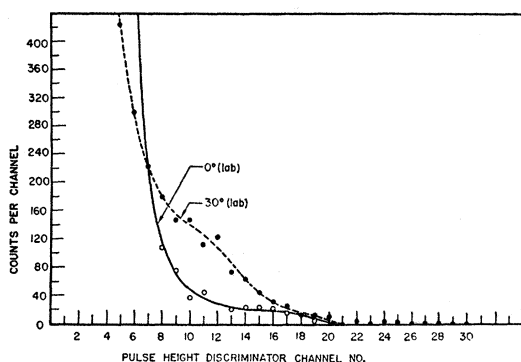


FIG. 5. $C^{13}(d,n)N^{14}$ pulse-height spectra.

made at equal angles on either side of 0° . These measurements also agree within statistical error.

At each angle the detector output was transformed into an energy spectrum by the pulse-height analyzer. A background run was carried out with only the target frame and tantalum backing foil in place. All data have been corrected for this background.

III. RESULTS

Four acceptable runs were taken on the $C^{13}(d,n)N^{14}$ reaction and three on each of $F^{19}(d,n)Ne^{20}$ and $Be^9(d,n)B^{10}$. Typical pulse-height spectra obtained with the pulse-height analyzer are shown in Fig. 5. Each of the runs corresponds to a total deuteron charge of 3.0×10^{-5} coulomb at each angle.

In order to identify the ground-state neutron group at each angle, the corresponding alpha-recoil energy was calculated. Since only the highest energy neutrons from each reaction were of interest the variation of alpha-energy with recoil angle was neglected. It was thus possible to select a range of pulse heights corresponding to the neutron group under study. For the N^{14} , neutrons were accepted in the range 7.0 to 9.0 Mev; for Ne^{20} , in the range 11.75 to 13.5 Mev, and for B^{10} in the range 7.75 to 8.5 Mev. The total number of counts between these energy levels was proportional to the relative cross section at each angle and was plotted against the corresponding angle to give the observed angular distribution.

Because of the finite angular aperture of the detector it was necessary to apply a small correction to this observed distribution in order to obtain the "true" distribution in the laboratory system. Since the detector was symmetrical about a vertical median plane a "line" in the angular distribution would be observed as a symmetrical peak of width roughly equal to the chamber width. The correction was assumed to be equal to the second derivative of the observed distribution multiplied by a factor estimated from the detector geometry.¹² The largest such correction (7.5 percent) was at 0° in the $F^{19}(d,n)Ne^{20}$ distribution. For all other points the correction was less than the statistical error.

¹² H. Primakoff and G. Owen, Phys. Rev. **74**, 1406 (1948).

All distributions were transformed to the center-of-mass system for comparison with the Butler theory. Figure 6 shows the $F^{19}(d,n)Ne^{20}$ and the $Be^9(d,n)B^{10}$ distributions. The angular distribution for the $C^{13}(d,n)N^{14}$ neutrons and the $C^{13}(d,p)C^{14}$ protons were normalized to the same peak height and are plotted together in Fig. 7 for comparison.

The predicted angular distributions of the neutrons in the center-of-mass system were calculated from Eq. (34) in Butler's paper.⁷ The curves were calculated specifically for the $C^{13}(d,n)N^{14}$ reaction assuming a Q of 5.38 Mev and an r_0 of 4.3×10^{-13} cm.

These curves are qualitatively correct for the Be^9 and F^{19} results. Figure 8 shows these curves normalized to the same peak heights as the experimental distributions.

Comparison of the $C^{13}(d,n)N^{14}$ experimental results with the predicted distributions indicates a parity change and an angular momentum transfer of one unit. Consequently, the parity of N^{14} is opposite to that of C^{13} , hence even.

Similar comparisons indicate a parity change in the

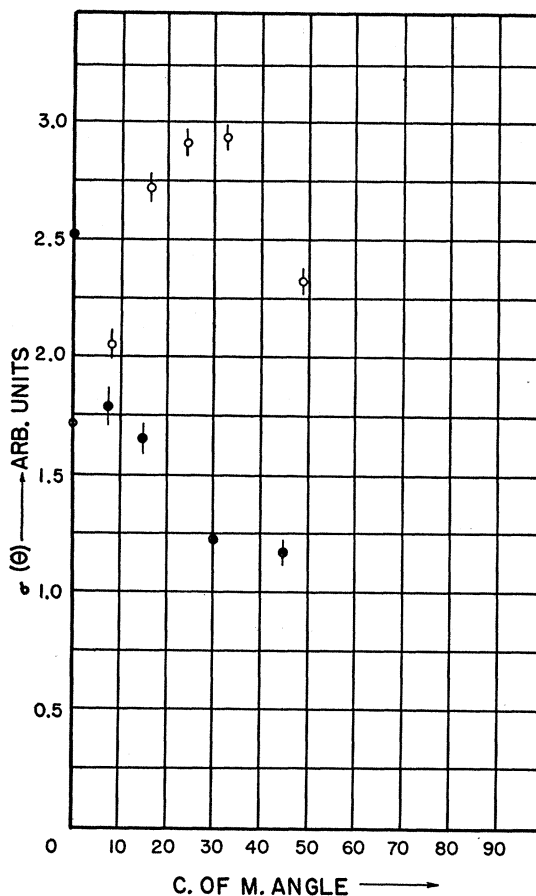


FIG. 6. The closed circles give the angular distribution of the neutrons from the $F^{19}(d,n)Ne^{20}$ ground-state reaction, and the open circles give the angular distribution of the neutrons from the $Be^9(d,n)B^{10}$ ground-state reaction (4-Mev deuterons).

$Be^9(d,n)B^{10}$ reaction and no parity change in the $F^{19}(d,n)Ne^{20}$ reaction. These latter results are considered as evidence supporting the validity of the N^{14} parity assignment. The forward maximum in the $F^{19}(d,n)Ne^{20}$ angular distribution is much less pronounced than that predicted. This may be due to the low deuteron energy and relatively higher Z . Ajzenberg has obtained a similar distribution for the $O^{16}(d,n)F^{17*}$ (536-kev level) transition using 3-Mev deuterons.¹³

IV. CONCLUSIONS

The B^{10} parity has been shown to be opposite to that of Be^9 , in agreement with previous results.¹⁴ The F^{19} parity has been shown to be the same as that of Ne^{20} and is therefore presumably even, in agreement with the predictions of the Mayer shell model.

The ground state of N^{14} has been shown to have even

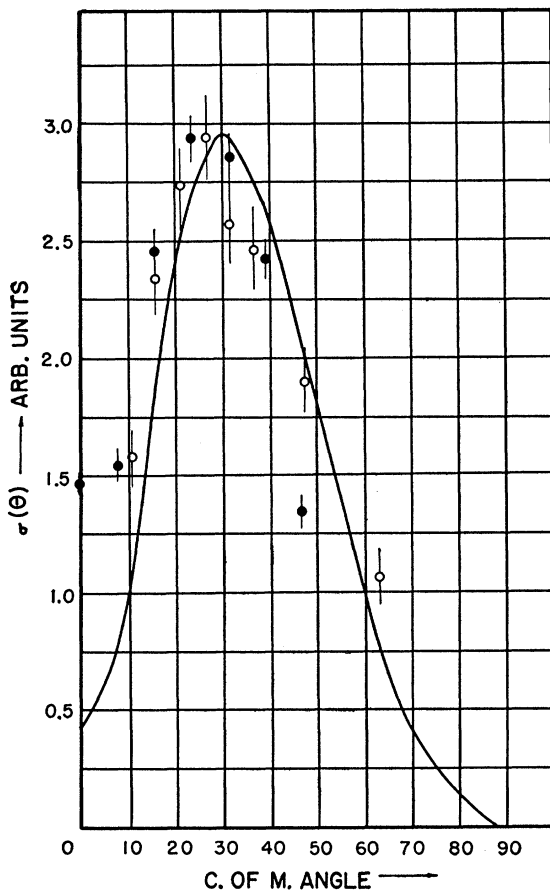


FIG. 7. The closed circles give the angular distribution of the neutrons from the $C^{13}(d,n)N^{14}$ ground-state reaction and the open circles give the angular distribution of the protons from the $C^{13}(d,p)C^{14}$ ground-state reaction, normalized to the same peak height. The theoretical curve $l_p=1$ (4.00 Mev) is included for comparison.

¹³ F. Ajzenberg, Phys. Rev. 83, 693 (1951).

¹⁴ F. Ajzenberg, Phys. Rev. 87, 205 (1952).

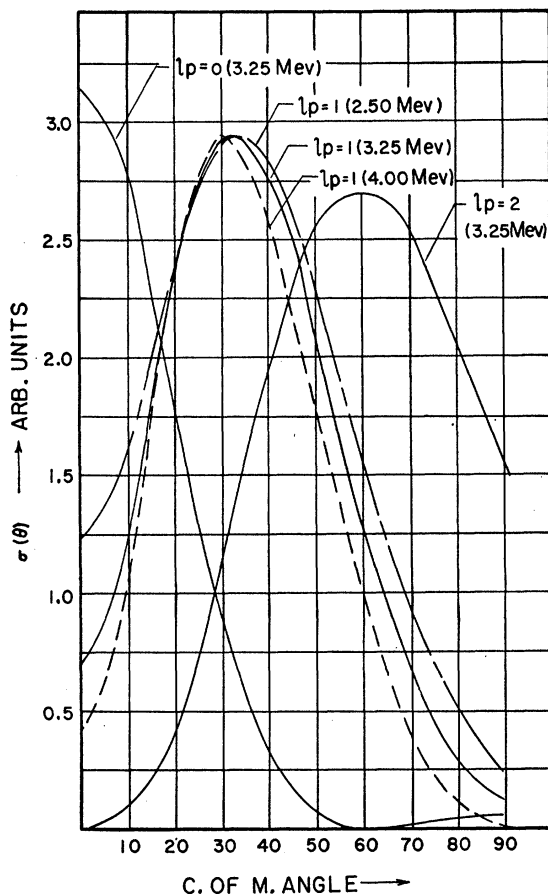


FIG. 8. Neutron angular distributions predicted by the Butler theory for the $C^{13}(d,n)N^{14}$ reaction. l_p is the angular momentum transferred to the target nucleus by the absorbed proton. The indicated energies are the laboratory energies of the deuterons used in the calculations. The Q value assumed was 5.38 Mev and r_0 was taken as 4.3×10^{-13} cm.

parity. This result is also in agreement with the predictions of the shell model.

Since the study of the $N^{14}(d,p)N^{15}$ reaction¹⁵ has shown a parity change, this work shows that N^{15} has odd parity.

The agreement between the neutron and proton angular distribution in Fig. 7 indicates that for 4-Mev incident deuterons, the Coulomb effects on the angular distribution of the emitted nucleon are relatively unimportant. Finally, and most important, this agreement is conclusive evidence that there is no parity change in the C^{14} beta-decay.

The author wishes to express his gratitude to Professor H. W. Fulbright for suggesting the problem and for his very valuable advice and assistance. He also wishes to thank Mr. L. M. Goldman for his cooperation during the course of the experiment.

He is indebted to the National Research Council of Canada for the award of a Special Scholarship during the early stages of this work.

¹⁵ J. Rotblat, as quoted by S. T. Butler (reference 7).

APPENDIX I Target Preparation

Barium carbonate, enriched to 53.7 percent C^{13} , was obtained from the Eastman Kodak Company, Rochester, New York, and was reduced to the elemental form by means of a technique similar to that used by Anderson *et al.*¹⁶ for the production of C^{14} samples.

The barium carbonate was doubly decomposed with lead chloride, to yield carbon dioxide, by prolonged heating at 360°C in a potassium nitrate and sodium nitrate bath. The fine magnesium turnings and cadmium metal catalyst were contained in a stainless steel reaction boat in a stainless steel furnace. The reduction reaction was initiated by flaming the furnace with a gas-oxygen torch and was completed, over a period of several hours, by maintaining the furnace at about 1000°C with an external electric heater.

The resultant mixture of carbon, magnesium oxide, and magnesium metal was treated with boiling concentrated hydrochloric

¹⁶ Anderson, Arnold, and Libby, *Rev. Sci. Instr.* **22**, 225 (1951).

acid, washed, and the filtrate was removed using a sintered glass filter and aspirator. This was repeated three times with concentrated hydrochloric acid and three more times with concentrated nitric acid. The carbon residue was evaporated to dryness, finely ground in an agate mortar, and weighed. An 80 percent recovery efficiency was found; the 20 percent loss was largely mechanical resulting from the difficulty in completely recovering the charge from the furnace and from the considerable handling which followed.

Tantalum foil of 0.003-inch thickness was used as a target backing because of its availability, high Z , and consequent low yield of neutrons from low energy deuteron bombardment. In preparing the C^{13} target it was found that if the fine carbon powder was made into a slurry with benzene and spread evenly on the tantalum, foil it did not crack or separate from the backing when the benzene was slowly removed by evaporation. This method was used to prepare a target of areal density 20 mg/cm². The Be^9 target consisted of a sheet of beryllium metal $\frac{1}{16}$ -inch thick. The F^{19} target consisted of a 0.012-inch sheet of Teflon (CF_2).

Properties of the Cr^{+++} Ion in the Paramagnetic Alums at Low Temperatures*

RALPH P. HUDSON

National Bureau of Standards, Washington, D. C.

(Received July 14, 1952)

Formulas for the entropy and magnetic moment as functions of temperature and magnetic field are derived for the paramagnetic chromic alums at liquid helium temperatures, taking into account the Stark splitting of the magnetic energy levels by the electric field of the crystal lattice. A comparison is made between values of the magnetic moment derived therefrom and the results of recent experimental work on paramagnetic saturation in potassium chromic alum by Henry.

I. INTRODUCTION

IN experiments on the magnetic properties of matter below 1°K it is often necessary to calculate the entropy of the paramagnetic salt as a function of external magnetic field at constant temperature, the adiabatic-demagnetization starting temperature. One makes use of the thermodynamic relation $(\partial S/\partial H)_T = (\partial M/\partial T)_H$, whence

$$S = S_0 - S_m = S_0 - S_H, \quad T = R \log_e(2J+1) + \int_0^H \left(\frac{\partial M}{\partial T} \right)_H dH, \quad (1)$$

and for M as a function of T and H it is customary to use the Brillouin formula,

$$M = NgJ\mu \left[\frac{2J+1}{2J} \coth \frac{2J+1}{2J} a - \frac{1}{2J} \coth \frac{a}{2J} \right], \quad (2)$$

where $a = gJ\mu H/kT$, the symbols having their usual meanings. Since the orbital quenching is practically complete in the magnetic alums at liquid helium tem-

peratures, we have $J=S=3/2$ (for Cr^{+++}) and g has the value 2. Combining (1) and (2) we obtain, for Cr^{+++}

$$S/R = x \coth x - 4x \coth 4x + \log_e \sinh 4x - \log_e \sinh x, \quad (3)$$

where

$$x = \mu H/kT.$$

The fact that the ion, in zero field, is not in a $(2J+1)$ -fold degenerate state but has its degeneracy partly lifted by the Stark splitting due to the crystalline electric field, is taken into account by correcting S_0 to $S_0 - S_e$. Here, S_e is simply related to the Stark splitting δ , if the temperature is sufficiently high to bring one into the region of the "tail" of the zero-field specific heat curve. Thus, in the case of potassium chromic alum $\delta/k \sim 0.25$ degree,¹ and if $T=1^\circ K$ or higher $C_e/R = \frac{1}{4}(\delta/kT)^2$ and $-S_e/R = -\frac{1}{8}(\delta/kT)^2$. At 1°K, therefore, $-S_e/R = -0.00781$; actually, use of this approximation still introduces a small error, and exact calculation gives 0.00775.

Strictly speaking, however, the application of this correction is valid only up to quite small external fields, such that $\mu H \ll \delta$. In large fields, where $\mu H \gg \delta$, the effect of the Stark splitting is negligible and the

* Supported by the ONR, Contract NAonr 12-48.

¹ de Klerk, Steenland, and Gorter, *Physica* **15**, 649 (1949).